Published in final edited form as:
Nat Biotechnol. 2008 October ; 26(10): 1187–1192. doi:10.1038/nbt.1496.

Small-molecule inhibition of HIV-1 Vif

Robin Nathans[1], **Hong Cao**[1], **Natalia Sharova**[2], **Akbar Ali**[1], **Mark Sharkey**[2], **Ruzena Stranska**[2], **Mario Stevenson**[2], and **Tariq M Rana**[1,3]

1 *Chemical Biology Program, Department of Biochemistry and Molecular Pharmacology, University of Massachusetts Medical School, Worcester, Massachusetts 01605, USA*

2 *Molecular Medicine Program, University of Massachusetts Medical School, Worcester, Massachusetts 01605, USA*

Abstract

The HIV-1 protein Vif, essential for *in vivo* viral replication[1–4], targets the human DNA-editing enzyme, APOBEC3G (A3G)[5], which inhibits replication of retroviruses and hepatitis B virus[6,7]. As Vif has no known cellular homologs, it is an attractive, yet unrealized, target for antiviral intervention. Although zinc chelation inhibits Vif and enhances viral sensitivity to A3G[8], this effect is unrelated to the interaction of Vif with A3G. We identify a small molecule, RN-18, that antagonizes Vif function and inhibits HIV-1 replication only in the presence of A3G. RN-18 increases cellular A3G levels in a Vif-dependent manner and increases A3G incorporation into virions without inhibiting general proteasome-mediated protein degradation. RN-18 enhances Vif degradation only in the presence of A3G, reduces viral infectivity by increasing A3G incorporation into virions and enhances cytidine deamination of the viral genome. These results demonstrate that the HIV-1 Vif-A3G axis is a valid target for developing small molecule–based new therapies for HIV infection or for enhancing innate immunity against viruses.

Since the first cases of AIDS were identified in 1981, this disease has led to the death of >20 million people. Despite remarkable medical advances, the incidence of HIV-1 infections continues to rise throughout the world. Current anti-HIV-1 agents target mainly the HIV-1 reverse transcriptase or protease. However, viral resistance and the toxicity associated with inhibitors of these enzymes have created a need for more potent and safer therapies against other viral targets.

Vif is one of only six HIV-1 regulatory proteins[1]. To identify small molecules that antagonize HIV-1 Vif function in host cells, we developed a high-throughput screen involving fluorescence-labeled A3G (Supplementary Fig. 1 online). As Vif downregulates A3G levels in human cells[9], we reasoned that Vif-A3G interactions in host cells could be quantitatively monitored by expressing A3G labeled with a fluorescent tag. Our rationale was that when 293T cells are co-transfected with yellow fluorescent protein (YFP)-tagged A3G and HIV-1 vectors with and without Vif (the subgenomic proviral vector pNL-A1 harboring HXB2 strain Vif and the corresponding Vif-deleted vector pNL-A1Δ*vif*, respectively), YFP fluorescence should be less in cells co-expressing A3G-YFP and wild-type HIV than in cells co-expressing A3G and Vif-deleted HIV. Moreover, a potential Vif inhibitor should reduce Vif downregulation of A3G-YFP, resulting in increased YFP signal intensity.

Correspondence should be addressed to M.S. (E-mail: Mario.stevenson@umassmed.edu) or T.M.R. (E-mail: trana@burnham.org).
[3]Present address: Program for RNA Biology, Sanford Children's Health Research Center, Burnham Institute for Medical Research, 10901 North Torrey Pines Road, La Jolla, California 92037, USA.

Note: Supplementary information is available on the Nature Biotechnology website.

Using this assay, we screened a diverse library of 30,000 small molecules and identified 537 compounds as primary hits. To exclude false-positive hits, these 537 compounds were retested in duplicate in a secondary screen. This second screen, which evaluated small molecules not only for reproduction of Vif inhibition, but also for inherent fluorescence, ability to increase general transfection and ability to increase nonspecific protein expression (in an red fluorescent protein (RFP)-based assay), yielded 66 compounds. Based on the diversity of their chemical scaffolds, these small molecules were then divided into ten classes. From each of these ten classes, we selected the two or three small molecules exhibiting the best activity in the secondary screen (% Vif inhibition). Structures of these 25 compounds, labeled RN-1 through RN-25, are shown in Figure 1a, and their median inhibitory concentration (IC_{50}) values for inhibition of A3G degradation in 293T cells are shown in Figure 1b.

HIV-1 replication depends on Vif activity only in host cells that express A3G[5]. In contrast to these 'nonpermissive' cells, those not expressing A3G do not require Vif for HIV-1 replication and are known as 'permissive'. To determine whether the small compounds RN-1 to RN-25 inhibit Vif function in the context of viral replication, we examined the antiviral activities of these compounds against wild-type HIV-1 in nonpermissive cells (H9, CEM) expressing A3G and in permissive cells (MT4, CEM-SS), which do not express A3G. We reasoned that specific Vif antagonists with the desired inhibitory profiles would inhibit viral replication in a dose-dependent manner only in nonpermissive cells but not affect replication in permissive cells. Cells were infected with an X4-tropic HIV-1_{LAI} variant in the presence of varying concentrations of Vif inhibitors, and viral replication was assessed at 2-d intervals by reverse transcriptase activity in culture supernatants (Fig. 2). The viability of cells was also checked every other day, using MTT (3-(4,5-dimethylthiazol-2-yl)-2,5-diphenyl tetrazolium bromide) assays to evaluate the toxicity of Vif inhibitors. RN-18 neither inhibits cell growth nor exhibits toxicity at 50 or 100 μM (Supplementary Fig. 2 online). The majority of the compounds (RN-5,6,9,10,12,13,15,17,20,21,22,23 and 25) did not exhibit antiviral activity in either MT4 or H9 cells (IC_{50} values >50 μM). Some compounds (RN-2,3,4,8,24) exhibited antiviral activity in both permissive and nonpermissive cells, indicating that their effects were not related to Vif. Two compounds with closely related structures (RN-18,19) exhibited an antiviral profile consistent with a Vif-specific inhibition in that they affected viral replication only in nonpermissive cells. Because of its greater potency (IC_{50} values of 4.5 and 10 μM in nonpermissive CEM and H9 cells, respectively, and IC_{50} > 100 μM in permissive cells), RN-18 was selected for more detailed analysis. Representative inhibitory profiles of RN-18 in permissive and nonpermissive cells are shown in Figure 2. In the presence of the inhibitor, RN-18, reverse transcriptase activity in the nonpermissive H9 and CEM cells decreased substantially and in a dose-dependent manner (Fig. 2a,b and Supplementary Fig. 3 online). However, RN-18 did not significantly affect reverse transcriptase activity in the permissive cell lines MT4 or CEM-SS (Fig. 2c,**d**). RN-18 also exhibited antiviral activity in CEM-SS modified to stably express A3G but did not exhibit antiviral activity in the parental CEM-SS cell line (Supplementary Fig. 4 online). Thus, the ability of RN-18 to inhibit HIV-1 replication in nonpermissive cells, but not in permissive cells, suggests that it is a Vif antagonist.

To investigate the mechanism and specificity of RN-18 function, we determined the effect of RN-18 on A3G levels in virus-producing cells and in virus particles. To that end, 293T cells were co-transfected with a luciferase reporter HIV-1 (pNL4-3LucR$^-$E$^-$) and hemagglutinin (HA)-tagged A3G expression vectors in the presence or absence of 50 μM RN-18. A3G, Vif and HIV-1 expression levels were analyzed by immunoblotting with antibodies against the HA tag, HIV-1 Vif and the HIV-1 antigen p24, respectively. In cells treated with RN-18, Vif protein levels were downregulated, and A3G expression increased (Fig. 3a). Consistent with these findings, A3G incorporation into virions (Fig. 3b) was enhanced in the presence of RN-18, and Vif levels in virus were decreased, indicating that RN-18 inhibited Vif function and upregulated A3G levels.

To determine the effect of RN-18 on A3G abundance and virion incorporation in simian immunodeficiency virus (SIV)-1, we cultured 293T cells co-expressing SIV_{mac} 239 green fluorescent protein Δnef and HA-tagged A3G for 24 h in the presence (+) or absence (−) of 50 μM RN-18. Analysis of total producer cell lysates by immunoblotting with antibodies against the HA tag and SIV-1 antigen p27 showed increased A3G levels in the presence of RN-18 (Supplementary Fig. 5 online). SIV-1 virions from producer cell supernatants were concentrated, lysed and analyzed by immunoblotting. This showed that A3G incorporation in virions was also increased by RN-18 treatment (Supplementary Fig. 5). Together, these results indicate that the Vif antagonist, RN-18, increases A3G abundance in both SIV-1 producer cells and virions.

The human genome encodes seven APOBEC3 proteins from a single gene cluster located at chromosome 22 (ref. 10). Similar to A3G, APOBEC3F is a potent inhibitor of HIV-1 replication and is targeted by Vif. Although not as potent as A3G or APOBEC3F, APOBEC3C has been shown to inhibit HIV-1 replication. In contrast, APOBEC3B exhibits modest anti-HIV-1 activity relative to A3G and resists Vif because it does not interact with Vif in cells[6,11,12]. To determine the specificity of RN-18 function, we transfected 293T cells with a reporter HIV-1 (pNL4-3LucR^{-}E^{-}) vector and various HA-tagged APOBEC3 expression vectors in the presence or absence of 50 μM RN-18 and analyzed protein levels by immunoblotting. RN-18 significantly and quantitatively enhanced levels of A3G, APOBEC3F and APOBEC3C but had no significant effect on APOBEC3B abundance (Fig. 3c,d and Supplementary Fig. 6 online). Interestingly, Vif protein levels were downregulated in cells expressing A3G, APOBEC3F and APOBEC3C and did not change substantially when APOBEC3B was expressed. These results strongly suggest that RN-18 specifically inhibits Vif-mediated downregulation of APOBEC3 family members by decreasing Vif protein levels when Vif interacts with APOBEC3 proteins.

Our finding that RN-18 inhibited viral replication in nonpermissive cells, but not in permissive cells, suggests that RN-18 is a Vif-specific inhibitor of HIV-1 replication (Fig. 2). To assess whether RN-18 can restore A3G levels in nonpermissive cells in a Vif-dependent manner, we infected H9 and MT4 cells with wild-type HIV-1 (Fig. 4a) and Vif-deleted (*Δvif*) HIV-1 (Fig. 4b) in the presence and absence of RN-18, and analyzed the expression of A3G, Vif, p24 and cyclin T1 (internal control). The immunoblot results show that RN-18 increased A3G abundance by decreasing Vif levels only in nonpermissive H9 cells (Fig. 4a) and that this increase in A3G levels required Vif (compare Fig. 4a,b). Furthermore, RN-18 did not increase A3G abundance in uninfected cells (Fig. 4c). Together with the results shown in Figure 3, these results strongly suggest that RN-18 is a specific Vif antagonist that inhibits HIV-1 replication.

APOBEC3G is neutralized by HIV-1 through Vif[13–18], which functions in concert with an E3 ubiquitin ligase complex to mediate the polyubiquitination and rapid degradation of A3G through the proteasome[9,15,19–22]. The possibility that RN-18 modulates HIV-1 replication by inhibiting the general proteasome pathway in cells is not supported by our results in Figures 3 and 4a,b, which indicate that RN-18 specifically antagonizes Vif. Further support against this possibility is the exclusion of compounds that nonspecifically enhanced RFP expression during our secondary screening. To directly address whether RN-18 inhibits a general proteasome pathway, we treated cells with varying concentrations of RN-18 and analyzed levels of the cell cycle inhibitor, p21, expression of which is modulated by the proteasome[23]. RN-18 did not affect p21 expression, whereas the proteasome inhibitors MG132, ALLN and lactacystin increased p21 levels (Fig. 4d). In addition, pulse-chase kinetic experiments of Vif degradation revealed that RN-18 reduced Vif half-life from ~46 min to ~33 min only when A3G was present (data not shown). To further define the specificity of RN-18 in modulating A3G levels through a mechanism that depends on A3G-Vif interaction, we quantitatively analyzed the effect of RN-18 on the D128K mutant of A3G, which is not targeted

by Vif. RN-18 increased abundance of A3G-YFP, but not A3G-YFP (D128K), in HIV-1 producer cells (Supplementary Fig. 7 online). These results indicate that RN-18 is not a general proteasome inhibitor, but enhances A3G levels by specifically downregulating Vif when Vif interacts with A3G. RN-18 could directly disrupt Vif-A3G interactions leading to Vif degradation. Another plausible mechanism is that RN-18 interferes with Vif interaction with an adapter protein in the Vif-A3G–host protein complex making Vif less stable and enhancing its turnover. Further studies are required to understand the details of the molecular mechanism of RN-18 action.

To further understand the mechanism of antiviral function of RN-18, we determined the effect of RN-18 on both the packaging of A3G into virions and the editing function of A3G. First, 293 T cells co-expressing HIV-1 (pNL4-3LucR$^-$E$^-$) and various concentrations of A3G-HA (3.75, 7.5, 15 fmoles) were cultured for 24 h in the presence (+) or absence (−) of 50 μM RN-18. Protein contents and viral infections were analyzed as described above. In the presence of RN-18, increasing the amount of A3G vector (7.5–30 fmole) enhanced A3G expression in cell extracts, leading to less infectious virus (Supplementary Fig. 8a,c online). Control experiments showed that only 3.75 fmole of the A3G vector was sufficient for efficient A3G expression and its antiviral function (Supplementary Fig. 8b,d). These experiments indicate that the Vif antagonist, RN-18, enhanced A3G abundance in producer cells, resulting in less infectious HIV-1 virions. Similarly, HIV-1 virions obtained from H9 cells treated with RN-18 were less infectious (Supplementary Fig. 9 online). To analyze the editing function of A3G, we used a stable A3G-YFP–expressing cell line to produce wild-type or delta-Vif virions in the presence and absence of RN-18 and sequenced individual clones. This demonstrated that RN-18 enhances cytidine deamination of the viral genome (Supplementary Fig. 10 online). Taken together, these results demonstrate that RN-18 enhances A3G abundance and virion incorporation, which lead to the production of less infectious viruses mediated by the DNA editing function of A3G.

In summary, we have identified a lead compound that specifically antagonizes HIV-1 Vif function and inhibits viral replication by targeting the Vif-APOBEC3 axis. The pharmacological properties of this lead compound can be optimized and improved by analyzing the structure-function relationships governing inhibition of Vif function and target selectivity. Other than their medical applications, these pharmacological probes of Vif function can provide important new insights into the biology of HIV-1.

METHODS

Expression vectors

The HIV-1 subgenomic proviral vector pNL-A1 harboring HXB2 strain Vif, and the corresponding pNL-A1Δ*vif* were generous gifts of Klaus Strebel. HIV-1 luciferase reporter constructs pNL4-3LucR$^-$E$^-$ and pNL4-3ΔVif LucR$^-$E$^-$ were provided by Nathaniel Landau through the NIH AIDS Research and Reference Reagent Program, Division of AIDS, NIAID, NIH. APOBEC3G-YFP and APOBEC3G-HA were described previously[24,25]. The plasmid APOBEC3F-HA was a gift from Michael Malim, and plasmids APOBEC3B-HA and APOBEC3C-HA were generous gifts from Bryan Cullen.

High-throughput screening for Vif inhibitors

For the primary screen, 293T cells were seeded at 4×10^5 cells per well in 96-well plates (Greiner Bio-One) containing 158 μl Dulbecco's modified Eagle's medium (Invitrogen) supplemented with 10% FBS, and incubated overnight at 37 °C in a humidified incubator (5% CO_2). The next day, cells were transfected with 40 μl of a largescale Lipofectamine 2000 (Invitrogen)/DNA complex containing pNL-A1 (or pNL-A1 ΔVif) and pAPOBEC3G-YFP

(2:1 molar ratio) and incubated for 4 h at 37 °C in a humidified incubator (5% CO_2). Small molecules (2 μl) from a diverse library (Chembridge) were added to each well (final concentration, 50 μM in 1% DMSO), with the outside columns receiving 2 μl of DMSO for controls (final concentration, 1% DMSO for all wells). All plates were incubated as above for an additional 24 h. Cells were harvested by removing the entire supernatant and adding 100 μl Mammalian Protein Extraction Reagent (M-PER, Pierce) supplemented with 0.5% (vol/vol) Triton X-100 (Pierce), 150 mM NaCl, 5 mM EDTA and a 1:100 (vol/vol) dilution of a protease-inhibitor mixture for mammalian tissue. Cell extracts were mixed well and incubated for 1 h at 25 °C with shaking. YFP fluorescence was monitored using a Safire (Tecan) plate reader (excitation: 510 nM, emission: 525 nM). For secondary screening, the 'hits' from the primary screen were retested in duplicate (final concentration, 50 μM). Primary screen hits were also tested for inherent YFP fluorescence by adding 2 μl of the small molecule to 200 μl/well. Cell extracts were prepared and their YFP fluorescence was measured as above. Finally, primary screen hits were tested for their ability to increase general transfection and/or protein expression. 293T cells were transfected, treated, incubated and harvested as above, except dsRed plasmid (Clontech) was used for transfection and RFP fluorescence was monitored (excitation: 545 nM, emission: 620 nM). Except for cell seeding, all primary and secondary screening procedures were performed using a Te-MO (Tecan) automated system.

Dose response and IC_{50} values for Vif inhibitors

293T cells were seeded in 12-well plates containing DMEM supplemented with 10% FBS and incubated overnight at 37 °C in a humidified incubator (5% CO_2). Cells were transfected with pNL-A1 (or pNL-A1 ΔVif) and pAPOBEC3G-YFP (2:1 molar ratio) using Lipofectamine 2000 according to the manufacturer's instructions and incubated for 4 h at 37 °C in a humidified incubator (5% CO_2). Cells were then treated with compound RN-18 at final concentrations of 0, 3.125, 6.25, 12.5, 25, 50 and 100 μM (in 0.5% DMSO; Acros Organics) and incubated for 24 h at 37 °C in a humidified incubator (5% CO_2). Supernatants were removed from wells, and adherent cells were lysed for 30 min at 4 °C, with gentle mixing in 200 μl of M-PER supplemented with 0.5% (vol/vol) Triton X-100, 150 mM NaCl, 5 mM EDTA and a 1:100 (vol/vol) dilution of a protease-inhibitor mixture cocktail for mammalian tissue (all Sigma). Cell lysates were centrifuged for 5 min to remove insoluble material, and the supernatants were assayed for protein using the DC Protein Assay kit (Bio-Rad). YFP fluorescence was determined in triplicate for 60 μg protein/50 μl supernatant using the Safire plate reader. Vif inhibition at a given concentration of RN-18 was calculated as '% Vif activity' using the formula:

$$100 - [\mu\,\text{conc} - \mu - \text{ctl}/\mu + \text{ctl} - \mu - \text{ctl}] \times 100 = \%\,\text{Vif activity}$$

For range correction:

Inhibition data were set to a 2-parameter equation, with the lower data limit at 0, that is, the data are background corrected, and the upper data limit at 100, that is, the data are range corrected.

$$y = \frac{100\%}{1 + \left(\frac{x}{IC_{50}}\right)^{s}}$$

In this equation, s is a slope factor, y is Vif activity (%), and *x* is the drug concentration (μM). Grafit software was used to generate the fit to all curves and to determine IC_{50}.

Reverse transcriptase assay for HIV-1 replication

H9 or MT4 cells were maintained in RPMI Medium 1640 (Invitrogen) containing 25 mM HEPES and L-glutamine with 10% FBS, 100 units/ml penicillin, and 100 μg/ml streptomycin (Invitrogen) at 37 °C in a humidified incubator (5% CO_2). Cells were seeded at 2×10^5 per well in a 24-well plate, treated overnight with 0, 1, 5, 10, 25 or 50 μM RN-18 (all at 0.1% DMSO) and infected with HIV-1 (X4-tropic HIV-1 variant [HIV-1_{LAI}]) at 2×10^5 c.p.m. reverse transcriptase per well. All cells were maintained in the presence of DMSO or RN-18 for 14 d, and viral replication was monitored every 2 d by measuring reverse transcriptase activity in culture supernatants. The average % relative infectivity at day 7 was determined from 3 separate reverse transcriptase assays. Grafit software was used to fit curves and to determine IC_{50}.

Protein expression in producer cells and in virions

293T cells were co-transfected with 50 fmol pNL4-3LucR$^-$E$^-$ (with pVSVG at a 1:1 molar ratio) and APOBEC3G-HA using Lipofectamine 2000. For dose-response/specificity studies, cells were co-transfected with 50 fmol pNL4-3LucR$^-$E$^-$ or pNL4-3ΔVif R$^-$E$^-$ (with pVSVG at a 1:1 molar ratio) and 7.5 fmol APOBEC3G-HA, APOBEC3F-HA, APOBEC3B-HA or APOBEC3C-HA. At 4 h post-transfection, 0 or 50 μM RN-18 was added (all final 0.5% DMSO concentration) and cells were incubated for 24 h. Total cell lysates were prepared from producer 293T cells, and protein content was determined as above. Virions were collected from supernatants of 293T producer cells by centrifuging for 10 min at 500*g* and filtering through a 0.22-μ syringe filter. The virus concentration of each sample was determined by a p24 enzyme-linked immunosorbent assay kit (Zeptomatrix). An aliquot of supernatant was taken from each sample so that all samples would have the same final viral concentration in a minimal volume of lysis buffer. Briefly, supernatants were layered on top of 20% sucrose cushions and ultracentrifuged for 2 h at 90,017*g*. Virion particles were lysed using a minimal volume of M-PER supplemented with 0.5% (vol/vol) Triton X-100, 150 mM NaCl, 5 mM EDTA and a 1:100 (vol/vol) dilution of a protease-inhibitor mixture cocktail for mammalian tissue.

Protein expression was determined for each sample by immunoblotting. Producer cell lysates (20 μg) or virion lysates (100 ng) were denatured and reduced by adding 4 × SDS-PAGE sample buffer (50 mMTris-HCl, pH 6.8, 100 mM dithiothreitol, 2% (wt/vol) SDS, 0.1% (wt/vol) bromophenol blue, 10% (vol/vol) glycerol) followed by boiling for 5 min at 100 °C. Proteins were resolved by 12% SDS-PAGE and transferred onto a PVDF membrane (Bio-Rad) using a Semi-Dry Electroblotter (Bio-Rad). After transfer, the membrane was blocked overnight in 5% (wt/vol) nonfat dry milk in TBS-T (20 mM Tris, pH 7.4, 150 mM NaCl, 0.1% (vol/vol) Tween 20) and washed 3 times for 10 min each in TBS-T before and after adding antibody. All antibodies were diluted in 2.5% (wt/vol) nonfat dry milk in TBS-T.

APOBEC3G-HA, APOBEC3F-HA, APOBEC3B-HA, and APOBEC3C-HA were all detected with anti-HA rabbit polyclonal antibody (Santa Cruz Biotechnology) diluted to 0.02 μg/ml. Human CycT1 was detected with a goat anti-CycT1 polyclonal antibody (Santa Cruz Biotechnology) diluted to 0.1 μg/ml. HIV-1 p24 was detected in producer cell and virion lysates by using a p24 monoclonal antibody diluted 1:10,000. (This antibody was obtained from Michael H. Malim through the AIDS Research and Reference Reagent Program, Division of AIDS, NIAID, National Institutes of Health: HIV-1 p24 gag #24-4 monoclonal antibody [no. 6521]). All horseradish peroxidase-conjugated secondary antibodies were used at 0.05 μg/ml (Santa Cruz Biotechnology). Blots were developed with the BM Chemiluminescence Blotting kit (Roche Applied Science) and exposed to Kodak BioMax MR X-ray film (Eastman Kodak).

HIV-1 infection of H9 cells, RN-18 treatment and protein analysis

H9 cells were maintained in RPMI Medium 1640 containing 25 mM HEPES and L-glutamine with 10% FBS, 100 units/ml penicillin and 100 μg/ml streptomycin at 37 °C in a humidified incubator (5% CO_2). For infection, the virus equivalent of 1 μg (pNL4-3LucR$^-$E$^-$ or pNL4-3ΔVif LucR$^-$E$^-$ virus) was incubated with 3×10^5 H9 cells/well in 12-well plates and centrifuged at 500*g* for 90 min at 37 °C. Immediately after infection, cells were washed twice in 1× PBS and incubated for 48 h in complete H9 medium containing 0 or 50 μM RN-18 (all 0.5% DMSO final concentration).

For dose-response studies, H9 cells infected with 1 μg pNL4-3LucR$^-$E$^-$ virus were washed and incubated in completed medium containing 0, 12.5, 25 or 50 μM RN-18 (all 0.5% DMSO final concentration). H9 cells were incubated for 48 h at 37 °C in a humidified incubator (5% CO_2), collected by high-speed centrifugation, washed in 1× PBS and lysed in 100 μl modified M-PER solution as above. Lysis, electrophoresis and transfer procedures for H9 cells were similar to those for 293T cells. For western blot, procedures were identical to those for detection of human cyclinT1 and HIV-1 p24. Endogenous APOBEC3G was detected in H9 cells using a custom-maderabbit CQDL affinity-purified PcAb (Antibody Solutions) according to the manufacturer's recommendations. Vif was detected in infected H9 cells using mouse HIV-1 Vif monoclonal antibody #319 (obtained from Michael Malim through the NIH AIDS Research and Reference Reagent Program, Division of AIDS, NIAID, NIH) at a 1:1,000 dilution. Species-specific horseradish peroxidase-conjugated secondary antibodies were used at dilutions specified above and blots were developed as above.

Treatment of 293T cells, preparation of cell lysates, western blot, proteasome inhibitors

293T cells were co-transfected for 4 h with pNL4-3LucR$^-$E$^-$, pVSVG, and 15 fmol APOBEC3G-HA before adding 0, 3.125, 6.25, 12.5, 25 or 50 μM RN-18 (0.5% DMSO final concentration). 24 h after adding drugs, a total of 293T cell lysates (15 μg) were prepared and examined for APOBEC3G, Vif and cyclin T1 expression as described above. 293T cells were also transfected with pNL4-3LucR$^-$E$^-$, pVSVG and APOBEC3G-HA before adding 0 or 50 μM RN-18 (0.5% DMSO final concentration). To determine the effect of RN-18 on p21 levels, 293T cells were treated with 0, 3.125, 6.25, 12.5, 25 or 50 μM RN-18 for 24 h (all at 0.5% DMSO final concentration). Total cell lysates were prepared and their protein content quantified as above. An aliquot of each lysate (20 μg protein) was resolved by SDS-PAGE and transferred using standard semi-dry conditions. The cell cycle inhibitor, p21, was detected using a mouse anti-p21 monoclonal antibody (Santa Cruz Biotechnology) according to the manufacturer's instructions. As a control for RN-18 inhibition by a general proteasome-inhibitor pathway, 293T cells were treated for 8 h with 0 or 10 μM (final concentration) of a proteasome-inhibitor cocktail (MG132, ALLN, and lacatacystin in 0.5% DMSO final concentration). Samples were prepared, and p21 and cyclinT1 were detected as described above.

Supplementary Material

Refer to Web version on PubMed Central for supplementary material.

Acknowledgments

The HIV-1 subgenomic proviral vector pNL-A1 harboring HXB2 strain Vif, and the corresponding pNL-A1Δ*vif* were generous gifts of Klaus Strebel. HIV-1 luciferase reporter constructs pNL4-3LucR$^-$E$^-$ and pNL4-3ΔVif LucR$^-$E$^-$ were provided by Nathaniel Landau through the NIH AIDS Research and Reference Reagent Program, Division of AIDS, NIAID, NIH. The plasmid APOBEC3F-HA was a gift from Michael Malim, and plasmids APOBEC3B-HA and APOBEC3C-HA were generous gifts from Bryan Cullen. We also thank Rana laboratory members for helpful discussions and support and the University of Massachusetts Center for AIDS Research (CFAR) for virology support.

This work was supported in part by an NIH grant to T.M.R. and M.S. and by a Developmental award from the UMASS CFAR.

References

1. Gabuzda DH, et al. Role of vif in replication of human immunodeficiency virus type 1 in CD4+ T lymphocytes. J Virol 1992;66:6489–6495. [PubMed: 1357189]
2. Madani N, Kabat D. Cellular and viral specificities of human immunodeficiency virus type 1 vif protein. J Virol 2000;74:5982–5987. [PubMed: 10846079]
3. Strebel K, et al. The HIV 'A' (sor) gene product is essential for virus infectivity. Nature 1987;328:728–730. [PubMed: 2441266]
4. von Schwedler U, Song J, Aiken C, Trono D. Vif is crucial for human immunodeficiency virus type 1 proviral DNA synthesis in infected cells. J Virol 1993;67:4945–4955. [PubMed: 8331734]
5. Sheehy AM, Gaddis NC, Choi JD, Malim MH. Isolation of a human gene that inhibits HIV-1 infection and is suppressed by the viral Vif protein. Nature 2002;418:646–650. [PubMed: 12167863]
6. Cullen BR. Role and mechanism of action of the APOBEC3 family of antiretroviral resistance factors. J Virol 2006;80:1067–1076. [PubMed: 16414984]
7. Turelli P, Trono D. Editing at the crossroad of innate and adaptive immunity. Science 2005;307:1061–1065. [PubMed: 15718460]
8. Xiao Z, Ehrlich E, Luo K, Xiong Y, Yu XF. Zinc chelation inhibits HIV Vif activity and liberates antiviral function of the cytidine deaminase APOBEC3G. FASEB J 2007;21:217–222. [PubMed: 17135358]
9. Mehle A, Goncalves J, Santa-Marta M, McPike M, Gabuzda D. Phosphorylation of a novel SOCS-box regulates assembly of the HIV-1 Vif-Cul5 complex that promotes APOBEC3G degradation. Genes Dev 2004;18:2861–2866. [PubMed: 15574592]
10. Jarmuz A, et al. An anthropoid-specific locus of orphan C to U RNA-editing enzymes on chromosome 22. Genomics 2002;79:285–296. [PubMed: 11863358]
11. Doehle BP, Schafer A, Cullen BR. Human APOBEC3B is a potent inhibitor of HIV-1 infectivity and is resistant to HIV-1 Vif. Virology 2005;339:281–288. [PubMed: 15993456]
12. Langlois MA, Beale RC, Conticello SG, Neuberger MS. Mutational comparison of the single-domained APOBEC3C and double-domained APOBEC3F/G anti-retroviral cytidine deaminases provides insight into their DNA target site specificities. Nucleic Acids Res 2005;33:1913–1923. [PubMed: 15809227]
13. Mariani R, et al. Species-specific exclusion of APOBEC3G from HIV-1 virions by Vif. Cell 2003;114:21–31. [PubMed: 12859895]
14. Marin M, Rose KM, Kozak SL, Kabat D. HIV-1 Vif protein binds the editing enzyme APOBEC3G and induces its degradation. Nat Med 2003;9:1398–1403. [PubMed: 14528301]
15. Mehle A, et al. Vif overcomes the innate antiviral activity of APOBEC3G by promoting its degradation in the ubiquitin-proteasome pathway. J Biol Chem 2004;279:7792–7798. [PubMed: 14672928]
16. Sheehy AM, Gaddis NC, Malim MH. The antiretroviral enzyme APOBEC3G is degraded by the proteasome in response to HIV-1 Vif. Nat Med 2003;9:1404–1407. [PubMed: 14528300]
17. Stopak K, de Noronha C, Yonemoto W, Greene WC. HIV-1 Vif blocks the antiviral activity of APOBEC3G by impairing both its translation and intracellular stability. Mol Cell 2003;12:591–601. [PubMed: 14527406]
18. Zhang H, et al. The cytidine deaminase CEM15 induces hypermutation in newly synthesized HIV-1 DNA. Nature 2003;424:94–98. [PubMed: 12808465]
19. Conticello SG, Harris RS, Neuberger MS. The Vif protein of HIV triggers degradation of the human antiretroviral DNA deaminase APOBEC3G. Curr Biol 2003;13:2009–2013. [PubMed: 14614829]
20. Kobayashi M, Takaori-Kondo A, Miyauchi Y, Iwai K, Uchiyama T. Ubiquitination of APOBEC3G by an HIV-1 Vif-Cullin5-Elongin B-Elongin C complex is essential for Vif function. J Biol Chem 2005;280:18573–18578. [PubMed: 15781449]
21. Yu X, et al. Induction of APOBEC3G ubiquitination and degradation by an HIV-1 Vif-Cul5-SCF complex. Science 2003;302:1056–1060. [PubMed: 14564014]

22. Yu Y, Xiao Z, Ehrlich ES, Yu X, Yu XF. Selective assembly of HIV-1 Vif-Cul5- ElonginB-ElonginC E3 ubiquitin ligase complex through a novel SOCS box and upstream cysteines. Genes Dev 2004;18:2867–2872. [PubMed: 15574593]

23. Zavrski I, et al. Proteasome: an emerging target for cancer therapy. Anticancer Drugs 2005;16:475–481. [PubMed: 15846112]

24. Wichroski MJ, Ichiyama K, Rana TM. Analysis of HIV-1 viral infectivity factor-mediated proteasome-dependent depletion of APOBEC3G: correlating function and subcellular localization. J Biol Chem 2005;280:8387–8396. [PubMed: 15537645]

25. Wichroski MJ, Robb GB, Rana TM. Human retroviral host restriction factors APOBEC3G and APOBEC3F localize to mRNA processing bodies. PLoS Pathog 2006;2:e41. [PubMed: 16699599]

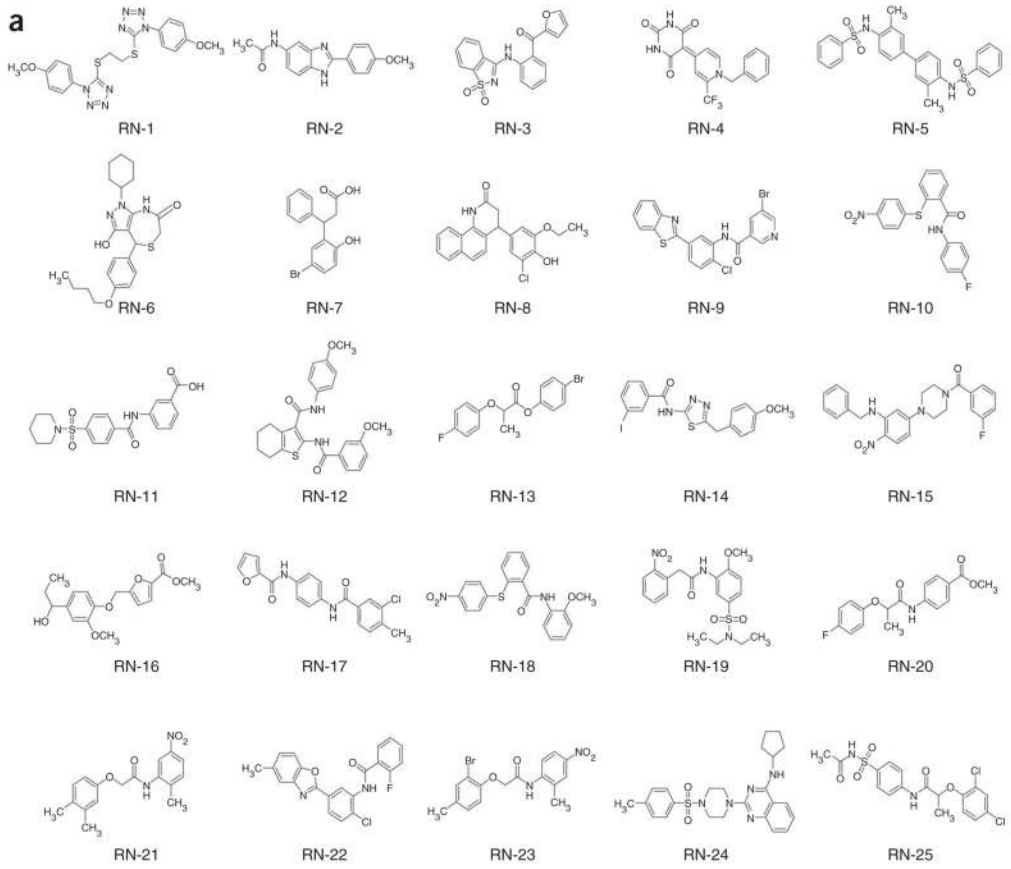

b

Small molecule	IC_{50}
RN-1	+
RN-2	+++
RN-3	++++
RN-4	+++
RN-5	++++
RN-6	+++
RN-7	+++
RN-8	+++
RN-9	++
RN-10	+++
RN-11	ND
RN-12	++++
RN-13	+++
RN-14	++
RN-15	++
RN-16	ND
RN-17	ND
RN-18	+++
RN-19	+
RN-20	ND
RN-21	ND
RN-22	+++
RN-23	ND
RN-24	++++
RN-25	ND

Figure 1.

Small molecules that inhibit HIV-1 Vif. (**a**) Small-molecule structures. Structures of small molecules isolated from a 30,000-compound library and exhibiting dose-dependent anti-Vif activities. (**b**) IC_{50} values. ++++, 0–10 μM; +++, 10 μM–30 μM; ++, 30–100 μM; +, >100 μM; ND, not determined.

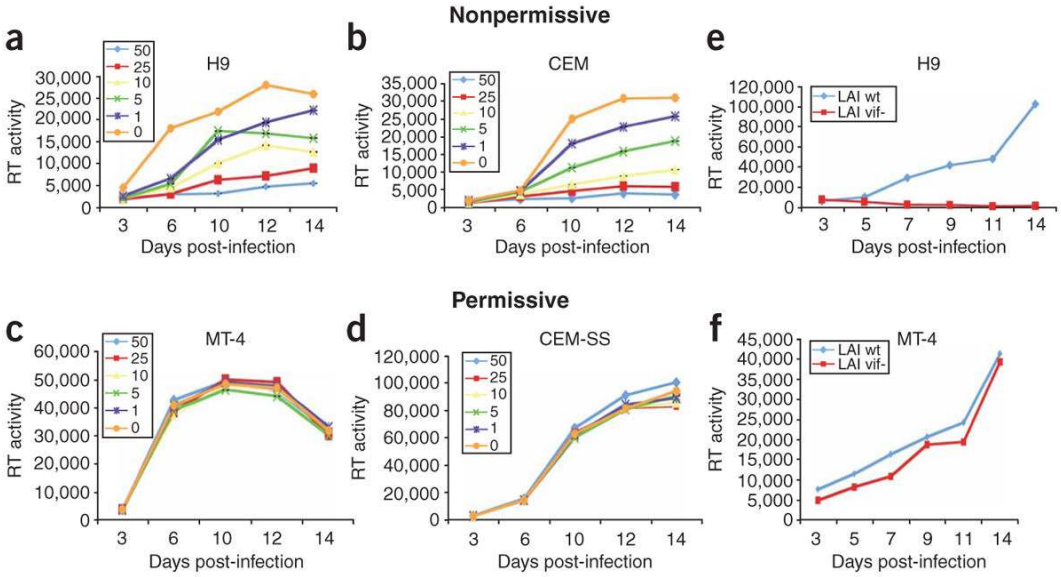

Figure 2.

The small-molecule Vif antagonist, RN-18, inhibits HIV-1 replication in nonpermissive cells but not in permissive cells. (**a**–**d**) CD^+ T-cell lines H9 (**a**), CEM (**b**), MT4 (**c**) or CEM-SS (**d**) were treated overnight with varying concentrations of RN-18 before infection with HIV-1 (X4-tropic HIV-1 variant [$HIV\text{-}1_{LAI}$]) at 2×10^5 c.p.m. reverse transcriptase (RT) per well. All cells were maintained for 14–21 d in the presence or absence of RN-18, and viral replication was monitored every other day by RT activity in culture supernatants. (**e**,**f**) For comparison, replication profiles of wild-type and Vif-deleted HIV-1 in nonpermissive (H9, **e**) and permissive (MT4, **f**) cells are shown.

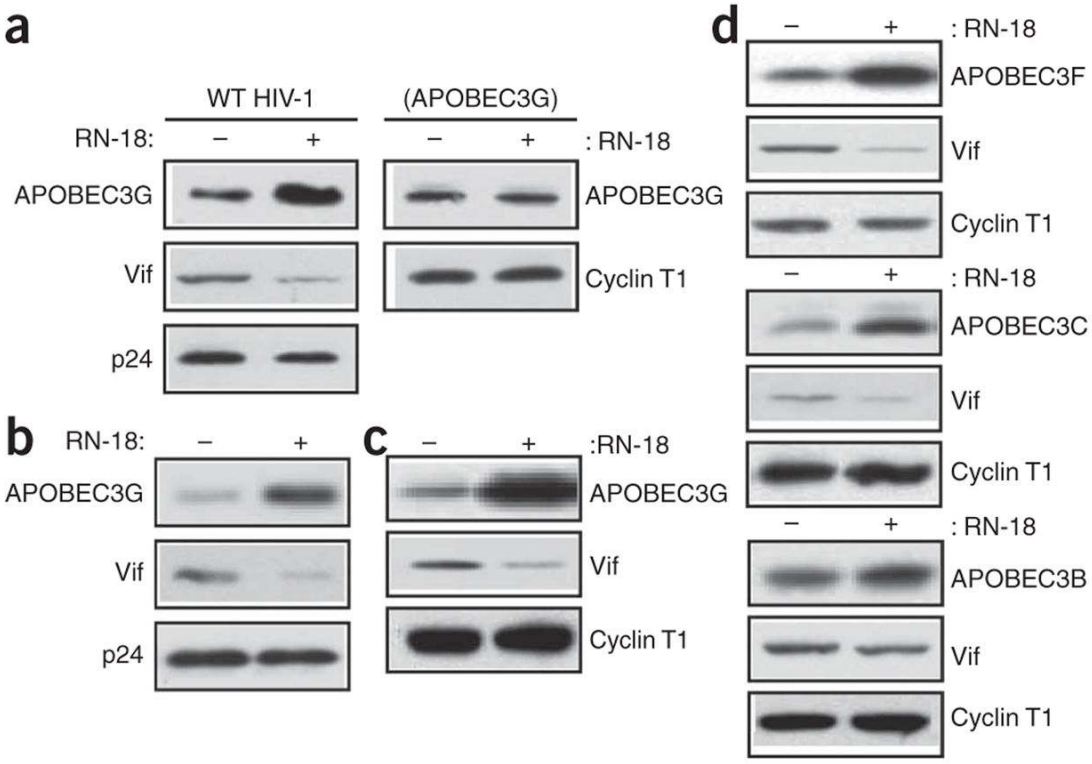

Figure 3.

The Vif antagonist, RN-18, increases APOBEC3G abundance in HIV-1 producer cells and virions, but does not affect APOBEC3B levels. 293T cells co-expressing HIV-1 (pNL4-3LucR^{-}E^{-}) and various HA-tagged APOBEC3 expression vectors were cultured for 24 h in the presence (+) or absence (−) of 50 μM RN-18. (**a**) Total producer-cell lysates were analyzed by immunoblotting with antibodies against the HA tag and HIV-1 antigen, p24. (**b**) HIV-1 virions from producer-cell supernatants were concentrated, lysed and analyzed by immunoblotting with antibodies against HA tag, HIV-1 Vif and p24. (**c**) Levels of APOBEC3G and APOBEC3F were determined by immunoblotting with antibodies against HA tag, Vif and cyclin T1 (internal control). (**d**) Levels of APOBEC3C and APOBEC3B were determined as previously specified.

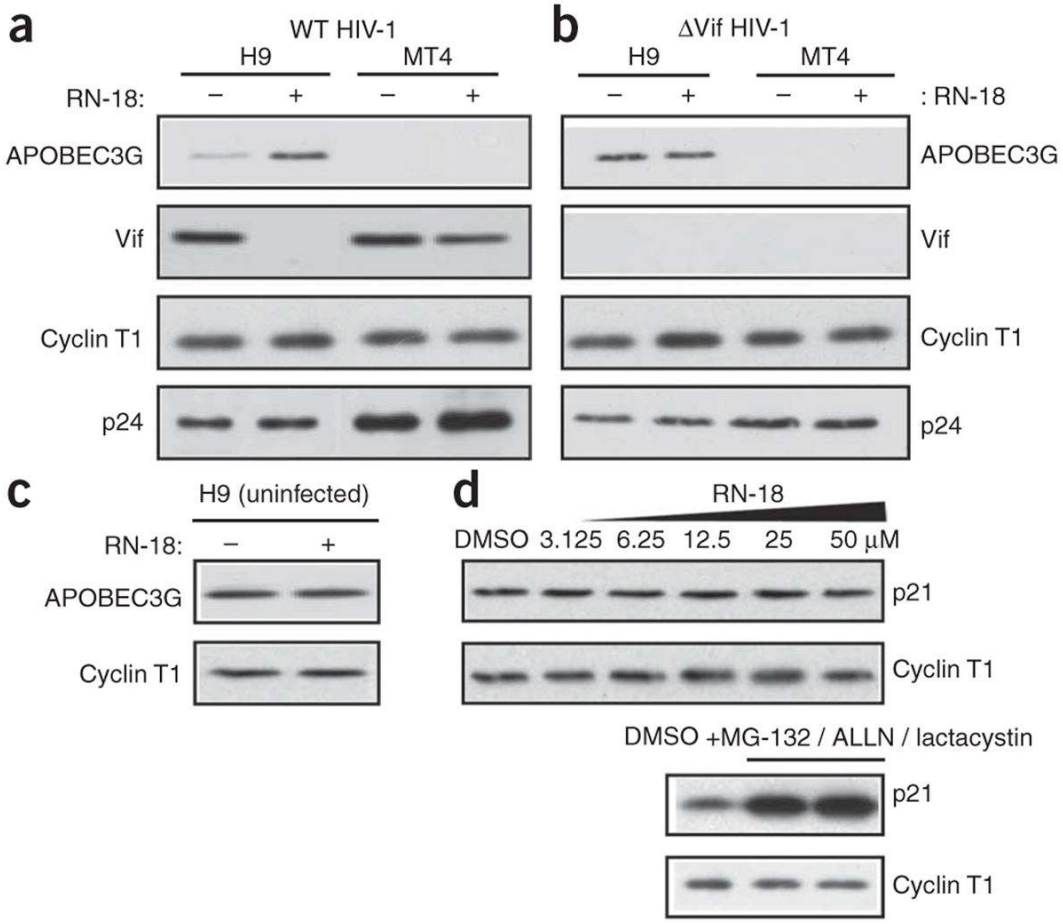

Figure 4.

The Vif antagonist, RN-18, enhances APOBEC3G expression in nonpermissive cells and in a Vif-dependent manner. (**a**,**b**) H9 (nonpermissive) and MT4 (permissive) CD^+ T-cells were infected with pNL4-3 $LucR^-E^-$ (**a**) or ΔVifpNL4-3 LucR-E (**b**) HIV-1. Immediately after infection, cells were washed and incubated for 48 h in complete medium containing 0 or 50 μM RN-18. Total cell lysates were analyzed by immunoblotting for cyclin T1, endogenous APOBEC3G, wild-type HIV-1 and p24. (**c**) RN-18 does not increase endogenous APOBEC3G levels in H9 cells. The nonpermissive H9 cells were incubated 48 h in complete medium containing 0 or 50 μM RN-18 and total cell lysates analyzed by immunoblotting for APOBEC3G and cyclin T1. (**d**) The Vif antagonist, RN-18, is not a general proteasome inhibitor. 293T cells were treated for 24 h with increasing doses of RN-18 (0 to 50 μM in 0.5% DMSO). Total cell lysates were analyzed by immunoblotting for cyclin T1 and the cell cycle inhibitor, p21. As a positive control (**d**), 293T cells were treated for 8 h with 0 or 10 μM of a proteasome inhibitor cocktail (MG132, ALLN and lacatacystin in 0.5% DMSO), and cell lysates were analyzed as in **c**.